Concentrated Gas Hydrate in the Shenhu Area, South China Sea: Results From Drilling Expeditions GMGS3 & GMGS4

Shengxiong Yang[1], Yong Lei[1], Jinqiang Liang[1], Melanie Holland[2]*, Peter Schultheiss[2], Jingan Lu[1], Jiangong Wei[1]
[1]Guangzhou Marine Geological Survey, China; [2]Geotek Ltd., United Kingdom
*Corresponding author: melanie@geotek.co.uk

Abstract

This paper provides a compendium of observations from boreholes in the Shenhu drilling area from Expeditions GMGS1, GMGS3, and GMGS4 regarding the gas hydrate concentration, morphology, composition, and distribution within the fine-grained sediments. Locations cored with gas hydrate zones showed concentrations of 20-60% (of pore volume) which varied from 10 m thick to over 80 m thick. Three locations re-occupied had extremely similar hydrate profiles, showing the area is locally homogenous. Two sites showed elevated salinities indicative of recent hydrate formation, and three sites had evidence of Structure II methane-propane hydrate.

Drilling for Gas Hydrate in the Shenhu Area, South China Sea

In 2007, the Guangzhou Marine Geological Survey (GMGS), the China Geological Survey (CGS) and the Ministry of Land and Resources of P. R. China completed Expedition GMGS1 in the Shenhu drilling area of the Northern South China Sea. Using the geotechnical drilling vessel Bavenit, eight sites were occupied for pilot hole/wireline logging operations. Five of these sites had offset holes drilled for core collection and *in situ* testing (Fig. 1). Three locations had meters-thick, relatively uniform sediment layers rich in gas hydrate located just above the base of gas hydrate stability. This gas hydrate was finely distributed within the foram-rich clayey silts, with concentrations from 20 to more than 40 percent of pore volume. The drilling results from the Shenhu area marked the first time that concentrated, disseminated gas hydrate had been observed in fine-grain sediments. [1, 2, 3]

Two recent expeditions were mounted to further explore the Shenhu gas hydrate province. Expeditions GMGS3 & GMGS4 took place in 2015 and 2016, respectively, both on the geotechnical drilling vessel Fugro Voyager. A logging-while-drilling (LWD) campaign began both expeditions, with 19 sites drilled in the Shenhu area on GMGS3 and 11 on GMGS4. A subset of these sites were revisited for coring and *in situ* testing later in the expeditions: four each on GMGS3 and GMGS4. Three of the coring locations on GMGS4 were near-reoccupations of locations cored on GMGS3 to characterize the local distribution of gas hydrate.

This paper is a summary of observations on gas hydrate from wells in the Shenhu drilling area from Expeditions GMGS1, GMGS3, and GMG4. The paper focuses on the locations that were cored, where hydrate was present: this includes boreholes GMGS1-SH2, -SH3, SH7; GMGS3-SH-W11-2015, -W17-2015, -W18-2015, -W19-2015; GMGS4-SH-W07-2016; and GMGS4-SC-W01-2017, -W02-2017, -W03-2017. For the purposes of this publication, in further references the borehole names have been shortened to provide clarity for the reader.

Shenhu Geological Setting

The Shenhu drilling area is located in the Pearl River Mouth Basin, in a deepwater depression known as the Baiyun Sag [4, 5, 6] (Fig. 1). The Baiyun Sag is a region of active deepwater hydrocarbon exploration with known gas reservoirs (e.g., [7]). Hydrocarbon reserves in the area have their source in mudstones & black shales of Eocene & Oligocene origin [8, 9], and there is a regional cap of Pliocene & Pleistocene marine clays & silts [10].

Locally, the bathymetry of the Shenhu drilling area is characterized by a migrating canyon system [11, 12]; the canyons and ridges are visible in Figure 1. Recent sedimentation is dominated by active downslope processes creating mass transport deposits, submarine fans, contourites, and turbidity channels [13, 14].

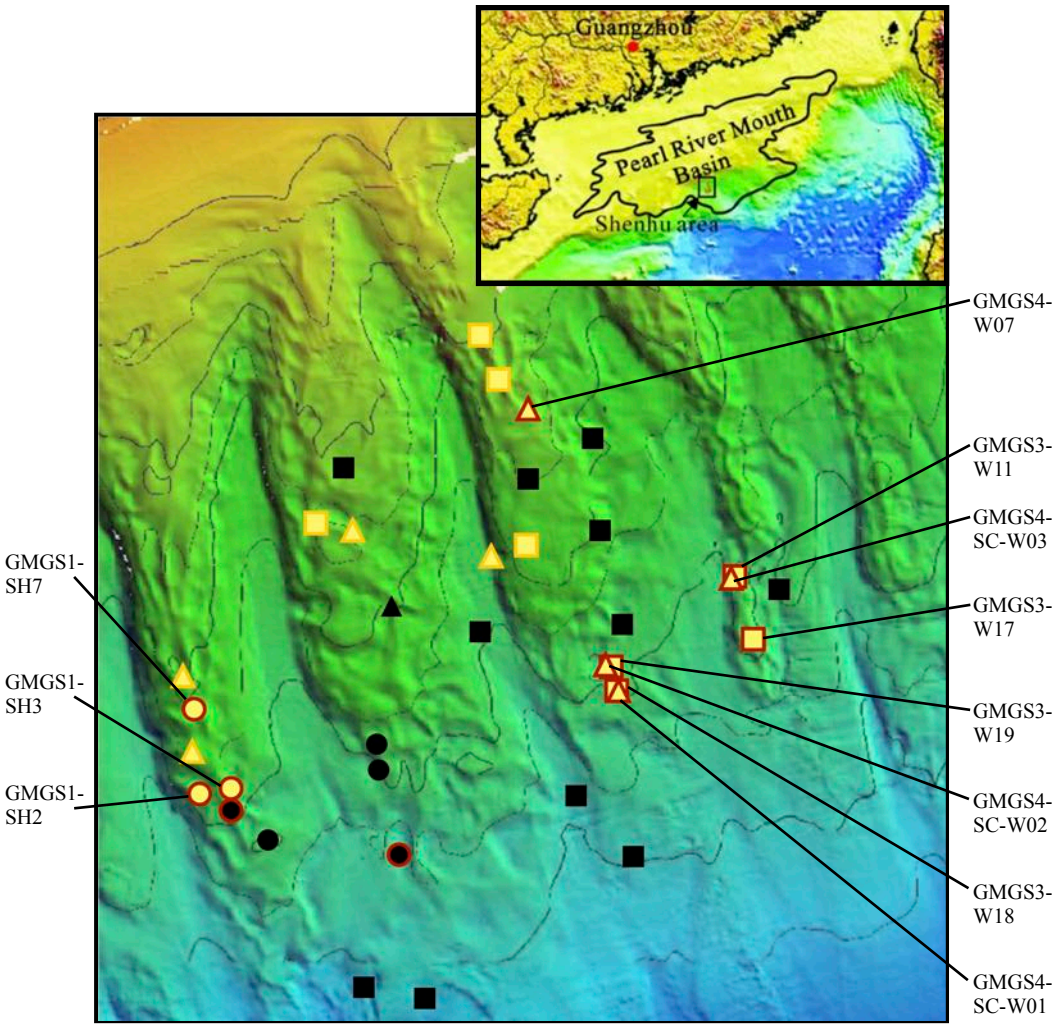

Figure 1: Location map of sites drilled in the Shenhu area on Expeditions GMGS1 (circles), GMGS3 (squares), and GMGS4 (triangles). Yellow locations showed evidence of gas hydrate; black locations did not. Red borders indicate locations where core samples were collected. Inset map shows the Shenhu area relative to the Northern South China Sea (after [Wang Collett 2014]).

Measurements Made During Expeditions GMGS1, GMGS3, & GMGS4

Borehole Logging

Borehole logging during Expedition GMGS1 was performed by Fugro Alluvial Offshore using the Antares slimline wireline logging tools. The tools were deployed inside the drill pipe to measure natural gamma, relative density, and relative neutron porosity, and deployed in an open-hole situation to measure natural gamma, density, neutron porosity, sonic velocity, formation resistivity, and fluid temperature and conductivity.

Logging-while-drilling (LWD) services were delivered by Schlumberger on Expedition GMGS3 & GMGS4. Schlumberger tools used included the GeoVISION, NeoScope, SonicScope (SonicVision), and ProVision tools which provide logs of gamma ray, resistivity, density, and neutron data, as well as resistivity imaging and compressional and shear-wave velocities.

Core Acquisition

Sediment samples on Expeditions GMGS1, GMGS3 & GMGS4 were collected through the use of both conventional wireline coring tools and pressure-retaining wireline coring tools. During GMGS1, conventional cores were collected with the Fugro Hydraulic Piston Corer “shoot sampler” (FHPC, ~8m) and the hammer-action Fugro Corer

(FC, ~2-m version). During GMGS3 & GMGS4, the FHPC was used as well as the rotary FMCB/FXMCB (Fugro [eXtended] Marine Core Barrel, ~4m).

Coring without release of *in situ* pressure was performed using the hammer action Fugro Pressure Corer (FPC) and the Fugro Rotary Pressure Corer (FRPC) during GMGS1. On GMGS3 & GMGS4, the FPC and the rotary PTCB (Pressure Coring Tool with Ball valve) were used for pressure coring.

In Situ Measurements

In situ temperature measurements are critical for studies involving gas hydrate to determine the base of gas hydrate stability. Measurements of *in situ* strength can be diagnostic of gas-hydrate-bearing sediments, and measurements of permeability are critical to understanding the dynamics of a gas hydrate system. During GMGS1, the temperature profile was determined from temperature measurements made using either the Fugro Wison EP temperature probe or the Fugro Pore Water Sampler (FPWS). On GMGS3, temperature measurements were made using the Fugro Temperature Cone Penetrometer (TCPT) and pore pressure dissipation tests were performed using the Fugro Piezo Cone Penetrometer (PCPT). Expedition GMGS4 used a combined tool to measure pore pressure dissipation, temperature, and cone strength: the Fugro Temperature-Piezocone Penetrometer Tool (TPCPT).

Measurements Under Pressure

Gamma density measurements, P-wave velocity measurements, and X-ray images of the FPC, FRPC, & PCTB pressure cores were collected using the Geotek PCATS (Pressure Core Analysis and Transfer System [15] on Expeditions GMGS1 & GMGS4. PCATS non-destructive data on pressure cores was collected for three basic purposes: to determine the nature and distribution of gas hydrate within the sediment core, to provide parameters for the mass balance calculations of gas from pressure cores, and to choose locations for subsampling under pressure (GMGS4 only).

Gamma density was measured with a ^{137}Cs source and a sodium iodide detector; the error in density was ±2%. P-wave velocity was measured using a pulse transmission technique at 250 kHz; the error in velocity was ±1%. X-ray images were collected with a microfocal source and a flat panel area X-ray detector with a pixel resolution of approximately 120 microns. Data in PCATS was collected at 0.5, 1 or 2 cm spacings. The centre 1 cm section from each X-ray image was concatenated to form a single image for each core.

Pressure Sample Depressurization & Mass Balance for Hydrate Quantification

Pressure cores or subsamples of pressure cores (GMGS4 only) were depressurised in a controlled fashion to accurately quantify the total amount of hydrocarbon gas in all phases, including gas hydrate. The pressure in the sample chambers was slowly and incrementally reduced through a manifold and expelled gas and fluid were collected at each pressure increment. Samples of gas were taken for analysis throughout the depressurisation process.

Gas collected during depressurisation was analysed using the on-board gas chromatograph to determine the composition of the gas released. Gas composition was measured using an Agilent MicroGC 3000 (GMGS1) or an Inficon Fusion MicroGC (GMGS3 & GMGS4) gas chromatograph with molecular sieve and PLOT U (GMGS1) or PLOT Q (GMGS3 & GMGS4) columns and thermal conductivity detectors. Oxygen, nitrogen, methane, ethane, and propane were measured on all expeditions, along with butane, isobutane, isopentane, and pentane during GMGS3 & GMGS4. The detection limit for all gases was 10 ppm; the quantification limit was 30 ppm.The total released volume of methane and other hydrate-forming gases was determined by measuring the volume of gas expelled from the system, adding the volume of fluid expelled from the system (trapped gas), and subtracting the compliance of the system. Total gas volumes were used to calculate notional *in situ* gas concentrations within the sediment, using the pore volume of the core. Pore volumes were calculated using length and diameter measured by X-ray under pressure and porosity calculated from density measured under pressure (assuming a grain density of 2.7 g/cm^3).

The calculated notional concentration of methane was compared to predicted methane concentration for *in situ* conditions [16] using measured *in situ* temperatures, measured baseline *in situ* salinities, and *in situ* pressures (assumed hydrostatic). Any methane present beyond dissolved methane concentration (“excess methane”) was assumed to be in a methane hydrate phase or a free methane gas phase, depending on the calculated thermodynamic phase boundaries. A hydration number of 6 (5.9 measured in [17]) and Structure I methane hydrate were assumed for these calculations, though these assumptions may not hold in all cases.

Infrared Imaging on Conventional Cores

Core temperature was measured in conventional cores to identify negative thermal anomalies created from dissociating gas hydrate. These measurements were used primarily as a tool to rapidly identify parts of the cores that contained, or had contained, gas hydrate, to direct further core sampling. Liner temperatures on FHPC, FC, FMCB, and FXMCB cores were measured as soon as the core was brought on board using a FLIR infrared (IR) camera on the Geotek MSCL-IR automated track to create a composite infrared thermal image.

Analysis of Porewater Freshening for Hydrate Quantification

Samples of all cores were taken for porewater analysis in sediments that might contain gas hydrate (negative thermal anomalies or high P-wave velocities under pressure) as well as in adjacent sediments with no evidence of gas hydrate. Porewater chloride concentration was measured on board by silver nitrate titration (error ±0.4 mM, GMGS1) or ion chromatography (error ±1.2 mM, GMGS3 & GMGS4).

To remove dilution of porewater by drilling fluids, sulfate was used as a tracer. All samples of interest were below the depth of zero sulfate in the sediments, and the drilling fluids contained sulfate due to use of seawater or addition of sodium sulfate. Reference samples of drill water were processed in the same manner as porewater samples and the drilling fluid signature was removed through a two-component mixing model.

Porewater freshening was calculated from the difference between measured chloride concentrations and the estimated *in situ* baseline chloride concentrations. As in Malinverno, et al. [18], the baselines were constructed using an empirical approach in which the *in situ* background chloride was defined to be the envelope of measurements around the discrete chloride anomalies. These discrete anomalies were used to estimate the gas-hydrate concentration [18]. Gas hydrate concentration has an estimated error of ±2% of pore volume (empirical estimate based on sediment sections containing no gas hydrate).

Gas Hydrate at the Shenhu Drilling Site

Concentration

The concentration of gas hydrate in the Shenhu sediments was calculated from methane mass balance in pressure core samples and porewater chloride freshening anomalies (Fig. 2). The same techniques have been used to calculate gas hydrate concentrations in sediments on the Cascadia Margin [19, 20], the Bay of Bengal [21, 22], and the Ulleung Basin [23, 24]. The maximum concentration of gas hydrate at the cored locations ranged from 25% to over 70% of pore volume, and at most sites the concentrations calculated from methane mass balance and the concentrations calculated from porewater freshening were in agreement. The gas hydrate concentrations were also coincident with anomalies in the electrical resistivity & sonic velocity downhole logs.

At two locations the gas hydrate concentrations calculated from methane mass balance and from porewater freshening did not match well (Fig. 3). These locations have significant uncertainties in their chloride baselines as they were cored incompletely, and no core was collected definitively below the zone of gas hydrate. The chosen baselines continue the trend of the sediments above the hydrate-bearing zone, but may overpredict the gas hydrate concentration. When compared to gas hydrate concentrations calculated from pressure core mass balance, the gas hydrate concentrations from porewater freshening are higher (Fig. 3). While the pressure cores can be used to help define the baseline chloride concentrations, for this presentation of the data the two methods have been kept independent to highlight any discrepancies.

For the bulk of the locations in the Shenhu area, the chloride baselines were approximated as simply as possible, with a straight line or simple curve, decreasing with depth. However, the GMGS4-SC-W01 & -W02 locations were an exception due to their unusual chloride profiles (Fig. 4). These two sites, which were within a kilometer of each other, show chloride steadily increasing toward the hydrate-bearing zone, indicating a source of salts within that zone. This chloride increase is consistent with ion exclusion due to hydrate formation [25], as seen in the sedimentary profiles at the Krishna-Godavari Basin [21], the Japan Sea [26], the Ulleung Basin [23], and Bullseye Vent [20]. The gas hydrate formation process at locations GMGS4-SC-W01 & -W02 may still be ongoing; alternately, the formation may have stopped but the salts have not had time to diffuse away [25]. These nearby locations have certainly been active more recently than any other site cored at Shenhu.

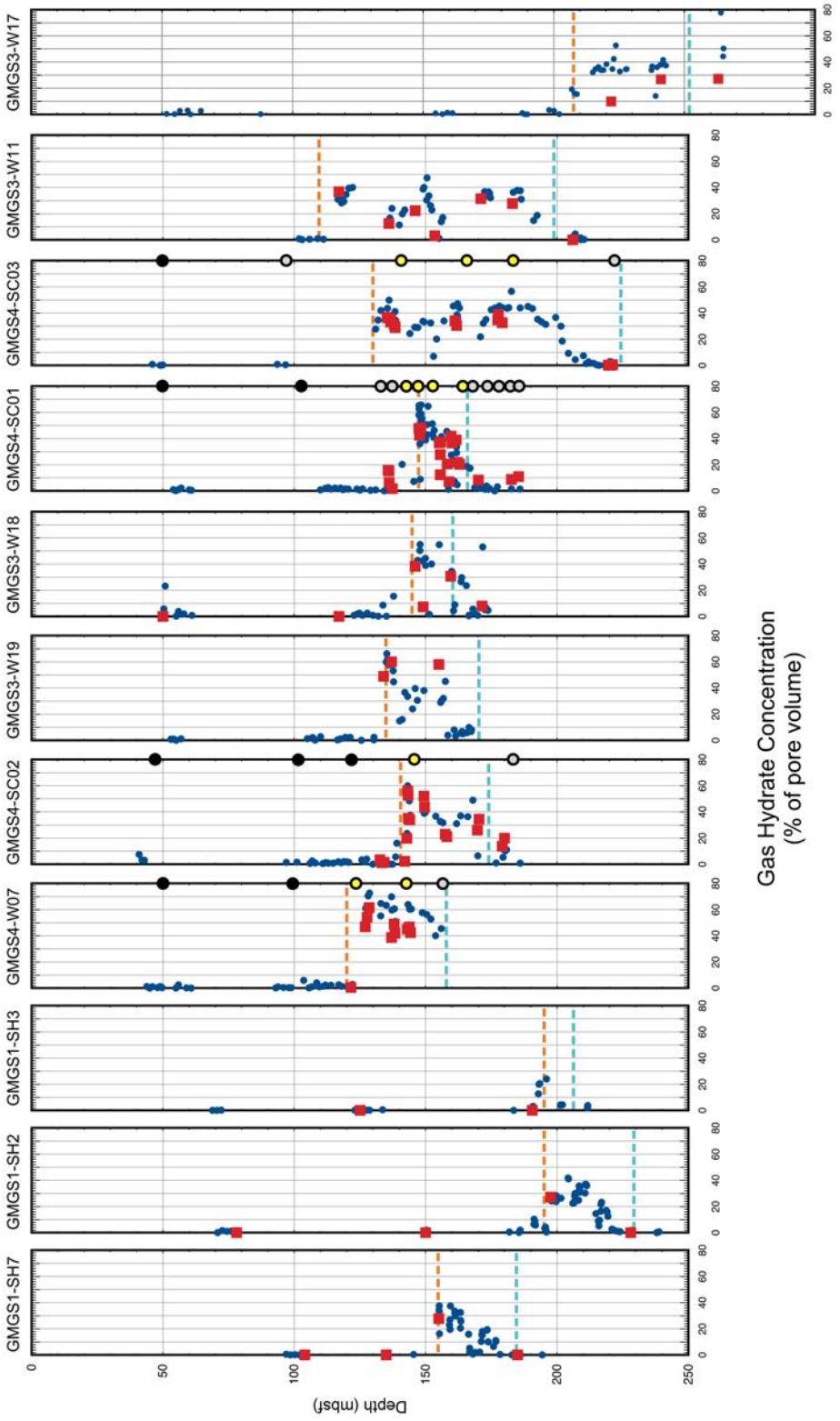

Figure 2: Gas hydrate concentration at eleven boreholes in the Shenhu area. Blue dots = gas hydrate calculated from porewater freshening; red squares = gas hydrate calculated from pressure core methane mass balance; orange dashed line = top of resistivity anomaly; blue dashed line = calculated base of gas hydrate stability (Structure I). Filled circles are locations with strength measurements < 5 MPa (black), < 10 MPa (grey), > 10 MPa (yellow).

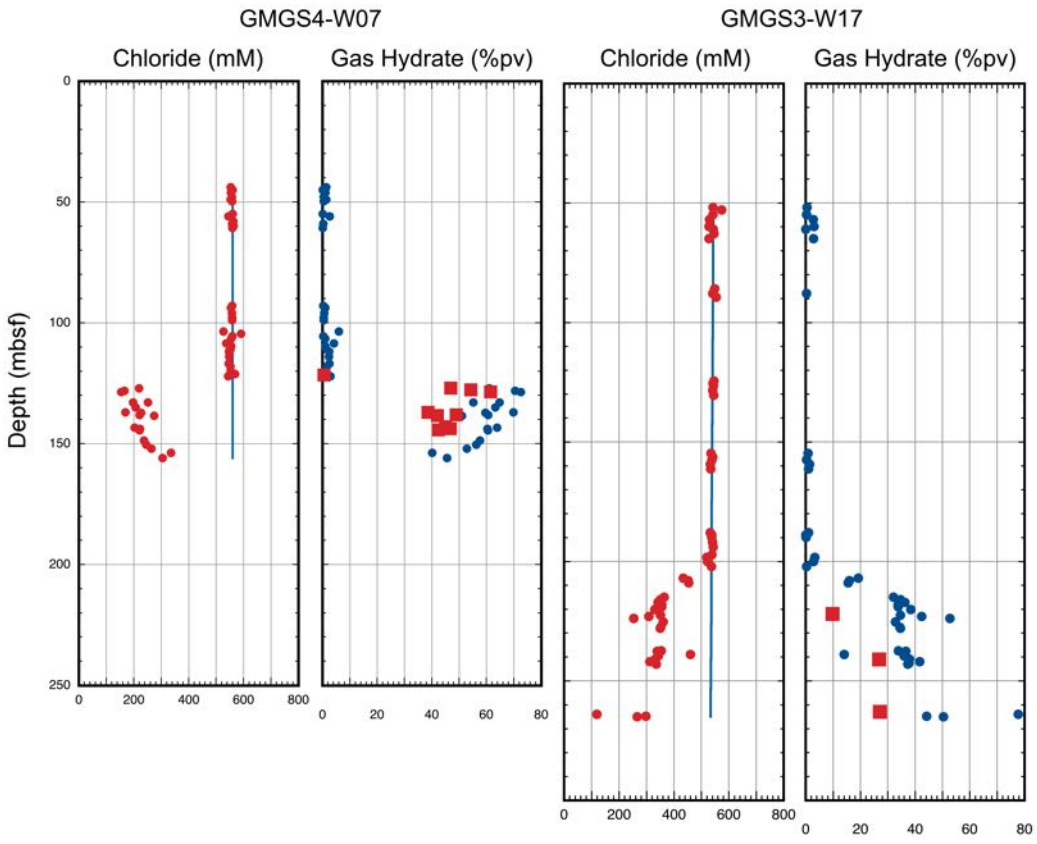

Figure 3: Chloride concentrations and calculated gas hydrate concentrations at two incompletely cored locations. Red circles = measured chloride concentrations, blue line = "envelope" of assumed baseline chloride concentrations. Circles = gas hydrate calculated from porewater freshening, squares = gas hydrate calculated from pressure core methane mass balance. % pv = % of pore volume.

Morphology

All the gas hydrate encountered was concluded to be of a disseminated, pore-filling nature. No gas hydrate in the form of veins, layers, or nodules could be seen visually in the conventional cores. All infrared thermal anomalies in conventional cores were diffuse, with no local cold spots.

The details of the PCATS nondestructive data collected under pressure provided further evidence that the morphology of the hydrate was finely distributed throughout the pore spaces. In general, grain-displacing gas hydrate structures, such as veins and lenses, are visible in density and X-ray data as low-density features and, if they are large enough, visible in the P-wave velocity data as high velocities [27]. Pore-filling disseminated gas hydrate is often not evident in density and X-ray data, as gas hydrate has a similar density to pore fluid, but can produce an anomalously high P-wave velocity if the sediment is cemented with gas hydrate [28]. All pressure core data from the Shenhu area (examples in Fig. 5) showed uniform densities and X-ray images, but elevated velocities (up to 2500 m/s) in cores containing gas hydrate (Fig. 6). The interpretation is that Shenhu sediments contain pore-filling gas hydrate cementing grains together.

Consistent with the interpretation of pore-filling, cementing gas hydrate, velocities also increased in downhole logs at the exact depth of the resistivity anomalies, and the sediment strength was higher in the gas-hydrate-bearing sediments [28]. A total of 29 *in situ* piezocone measurements (locations in Fig. 3) confirmed that the cone strengths inside the gas hydrate zones were 15-40 MPa, stiffer than sediments outside the gas hydrate zone (1-7 MPa).

Another confirmation of the gas hydrate morphology comes from the electrical resistivity downhole log data. Electrical resisitivity measured in wireline and LWD logs was elevated in the hydrate-bearing interval. The magnitudes of the resistivity anomalies at GMGS1-SH2 & -SH7, when converted to hydrate ("non-water")

concentrations via Archie's relation, matched the hydrate concentrations from core measurements [29]. Archie's relationship between resistivity and insulative material in pore space can only be successfully applied to formations with isotropic geometries. If the Shenhu gas hydrate were in veins or layers *in situ*, the resistivity anomalies would have been expected to be much larger (e.g., locations in the Krishna-Godavari Basin, [30] and any hydrate concentration calculated from Archie's relation would have been irreconcilable with core measurements [31].

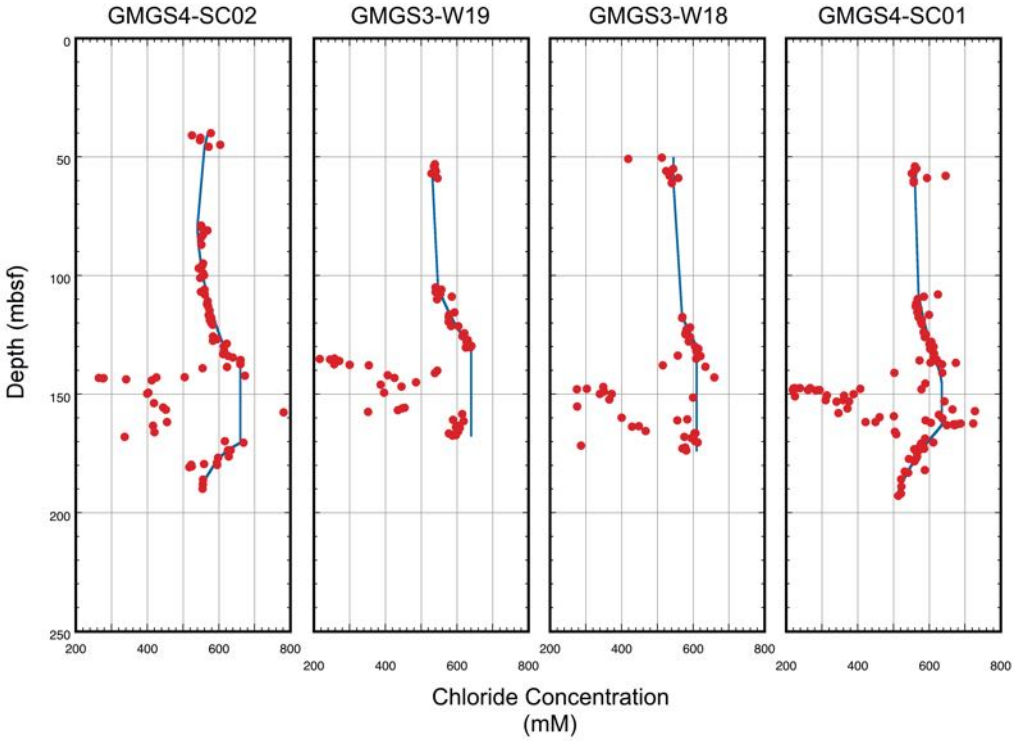

Figure 4: Chloride concentrations at four nearby boreholes, showing increased chloride in the middle of the sedimentary section. Red circles = measured chloride concentrations, blue line = "envelope" of assumed baseline chloride concentrations.

Composition

The hydrocarbon gases at the Shenhu area were predominantly methane, in both gas from sedimentary voids and from pressure core degassing. Ethane and propane were measureable in most samples of gas (Fig. 7), and showed strong trends related to the presence of gas hydrate. All locations showed increased concentrations of ethane in the gas-hydrate-bearing zone, and this increase persisted below the base of gas hydrate stability at most of the locations. Methane:ethane (C_1/C_2) ratios within the gas hydrate stability zone were mainly between 100-1000, which may be considered to indicate a gas of mixed microbial and thermogenic origin (e.g., [32]). Isotopic analysis of gases from pressure cores containing gas hydrate collected during GMGS1 also supported mixed origin for the gas, with $\partial^{13}C_{CH4}$ between -50‰ and -60‰ (PDB standard) [33].

Three locations had measured propane concentrations that were above 0.1%: GMGS4-SC-W01/GMGS3-W18, GMGS4-SC-W02/GMGS3-W19, and GMGS3-W17. When a gas mixture containing propane and methane forms gas hydrate, if the propane concentration is greater than 0.1%, the propane will force the gas hydrate into Structure II [34]. Therefore, it is likely that at least some of the gas hydrate at these sites was in the form of Structure II hydrate. Locations GMGS4-SC-W01/GMGS3-W18 and GMGS4-SC-W02/GMGS3-W19 also had butane, isobutane, and isopentane concentrations >100 ppm in the zone of gas hydrate occurrence (C_4+ not measured at GMGS3-W17).

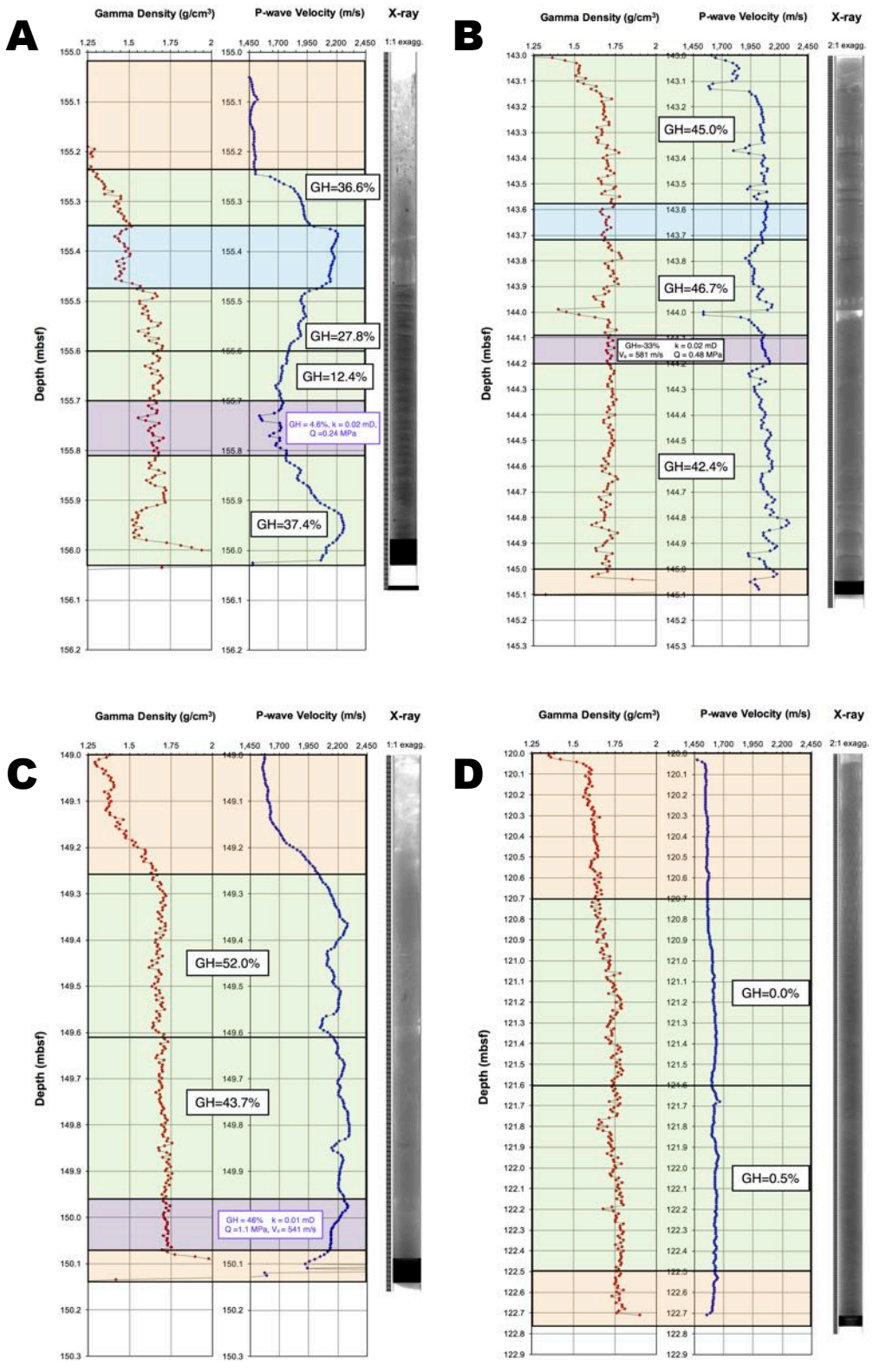

Figure 5: Summaries of nondestructive data collected under pressure on four pressure cores. A is from GMGS4-SC-W01, B is from GMGS4-SC-W02, and C & D are from GMGS4-W07. Cores were subsectioned under pressure, and green sections were depressurized for methane mass balance. Note high P-wave velocities in all cores except D, with no significant gas hydrate.

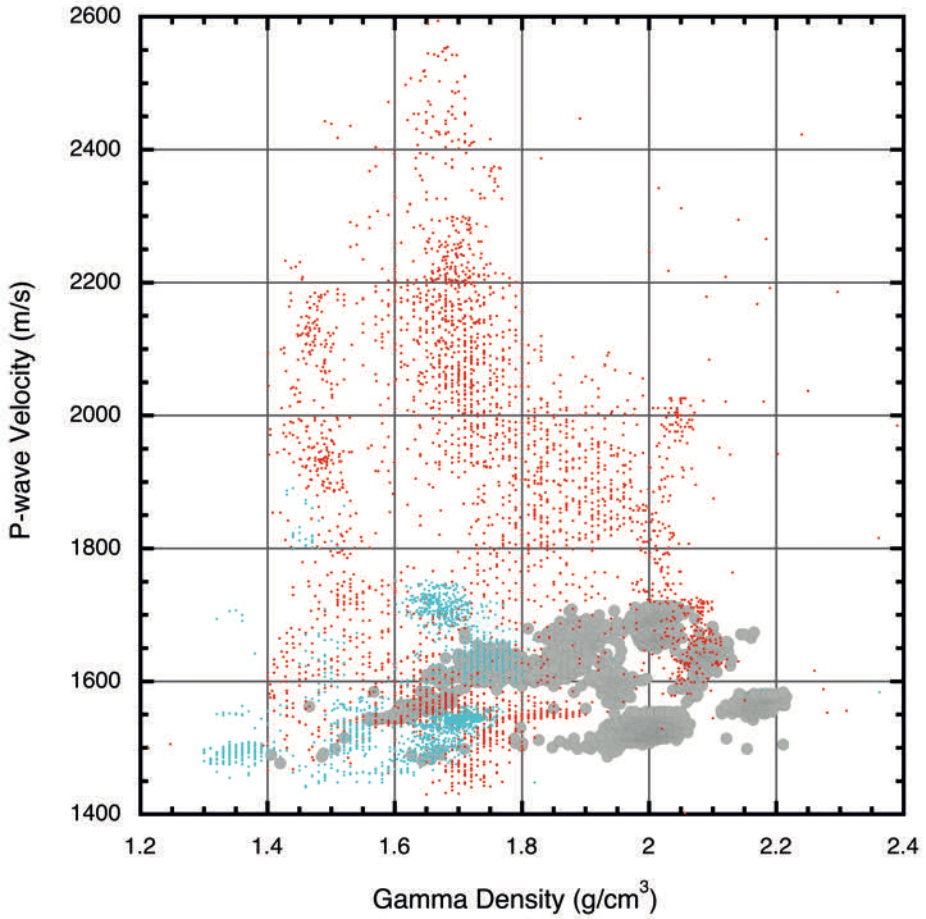

Figure 6: Cross-plot of density (as measured by gamma attenuation) and velocity for pressure cores from GMGS1 & GMGS4. Grey circles are from cores that contained no gas hydrate as measured by methane mass balance. Red dots are from cores that contained some high concentrations of gas hydrate; blue dots are from cores that contained only low concentrations of gas hydrate.

At the two locations which showed increased chloride in the gas-hydrate-bearing zone (GMGS4-SC-W01/GMGS3-W18 & GMGS4-SC-W02/GMGS3-W19), there were distinctive trends in C_2-C_5 gas concentration relative to the gas-hydrate-bearing zone (Fig. 8). Ethane decreased downhole to the top of the hydrate, and then increased in the hydrate-bearing zone. Isobutane, butane, and isopentane all showed an inverse profile to ethane. Propane generally increased with depth throughout both holes, but the maximum concentration was a spike near the top of the gas hydrate. These varied gases may give clues as to the formation and dissociation processes of the gas hydrate.

Distribution

The gas hydrate at most locations drilled in the Shenhu area follows a distinctive vertical pattern: there is a sharp top to the gas hydrate layer, and the concentrations in the layer decrease with depth until the base of Structure I methane hydrate stability is reached (Fig. 3). This creates a triangular profile that is visible in the graphs of gas hydrate concentration with depth and is also reflected in the electrical resistivity and sonic velocity downhole logs, not only at most of the locations cored, but also at locations with LWD data only. While some locations did not exhibit this triangular profile (most notably, the 80-meter-thick section at GMGS4-SC-W03/GMGS3-W11), the sharp top to the hydrate-bearing zone remains. The regional nature of this vertical character in the gas hydrate distribution must be a clue to the formation mechanism.

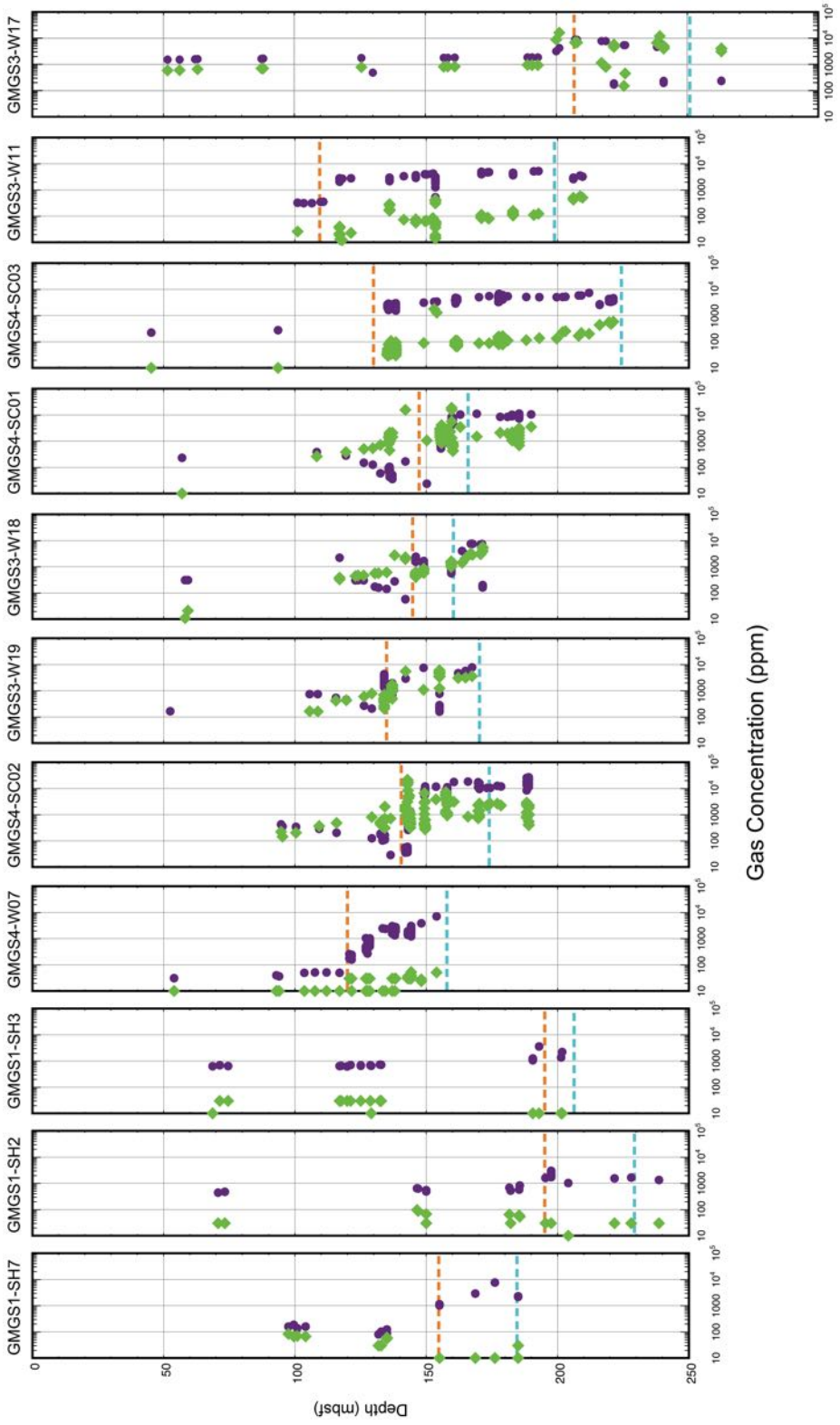

Figure 7: Gas composition from eight locations in the Shenhu area, from pressure cores and gas voids in conventional cores. Ethane concentration = purple; propane concentration = green; orange dashed line = top of resistivity anomaly; blue dashed line = calculated base of gas hydrate stability (Structure I)

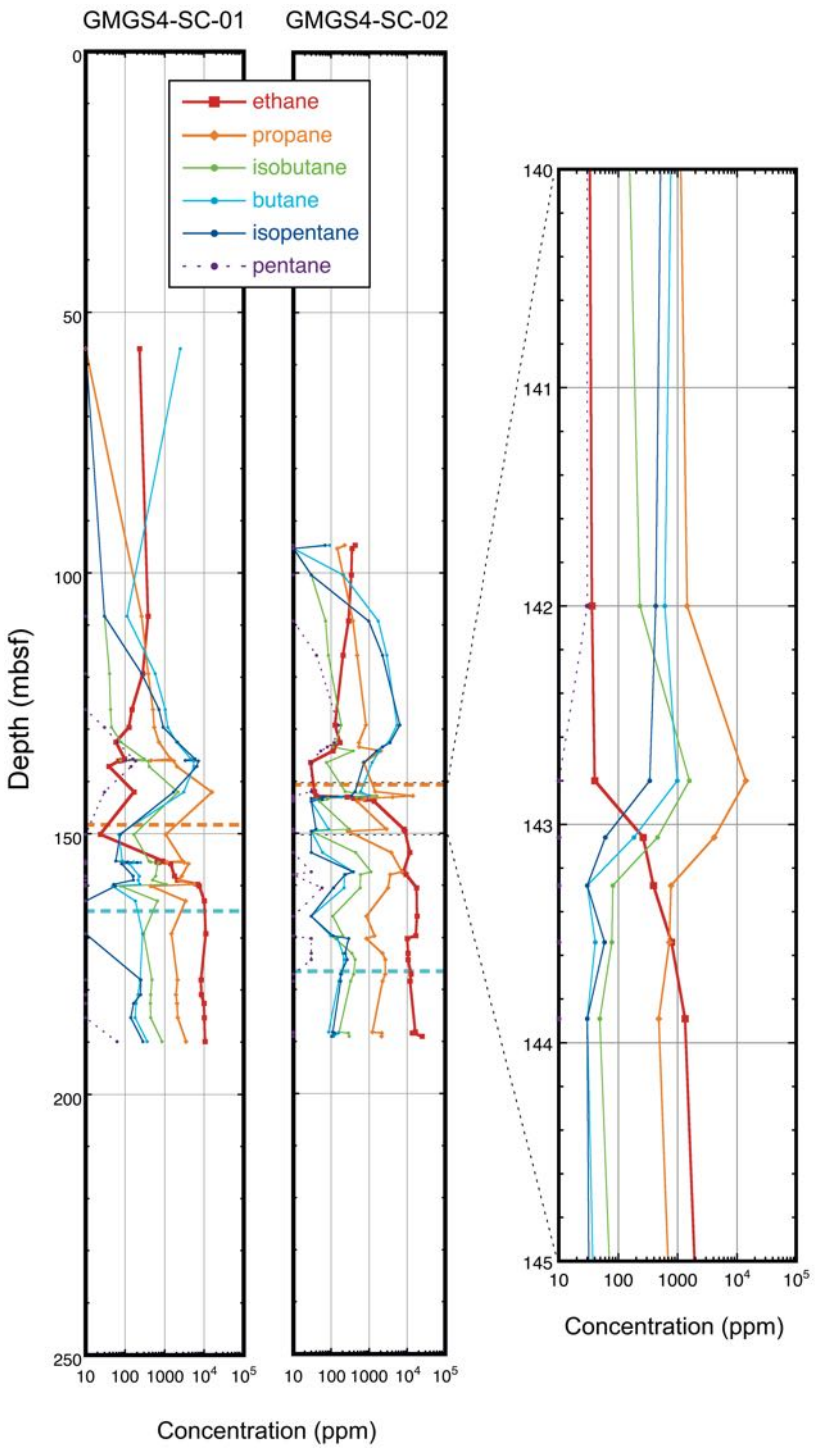

Figure 8: Gas composition from two nearby locations, from pressure cores and gas voids in conventional cores. Orange dashed line = top of resistivity anomaly in nearby LWD hole; blue dashed line = calculated base of gas hydrate stability (Structure I).

Three sites showed evidence for excess gas below the base of Structure I methane hydrate stability: GMGS4-SC-W01/GMGS3-W18, GMGS4-SC-W02/GMGS-W19, and GMGS3-W17. Pressure cores collected at each of these sites have excess methane beyond what can be dissolved in porewater, equivalent to methane hydrate at 10-25% of pore volume. While it is possible that some of this excess methane was present as free gas–though downhole log

data showed no signature low velocities–the composition of the gases at these locations (see **Composition**) indicate that Structure II methane-propane hydrate would also be a plausible explanation for this observation.

The lateral homogeneity of the Shenhu area was tested through the re-occupation of three sites cored on GMGS3 during GMGS4. Figure 9 compares the LWD data between these locations. Boreholes GMGS4-SC-W03 & GMGS3-W11 show an uncanny similarity in both the downhole log (Fig. 9) & core data (Fig. 3) sets. The other two pairs are also similar to each other, though the magnitudes of the anomalies do not match as well as at GMGS4-SC-W03/GMGS3-W11. The gamma ray logs at GMGS4-SC-W02 & GMGS3-W19 are quite different within the hydrate-bearing zone, and one interesting conclusion from this lateral exploration was that the low gamma ray sediments, composed in this case of carbonate rather than quartz, do not control the presence of gas hydrate at Shenhu.

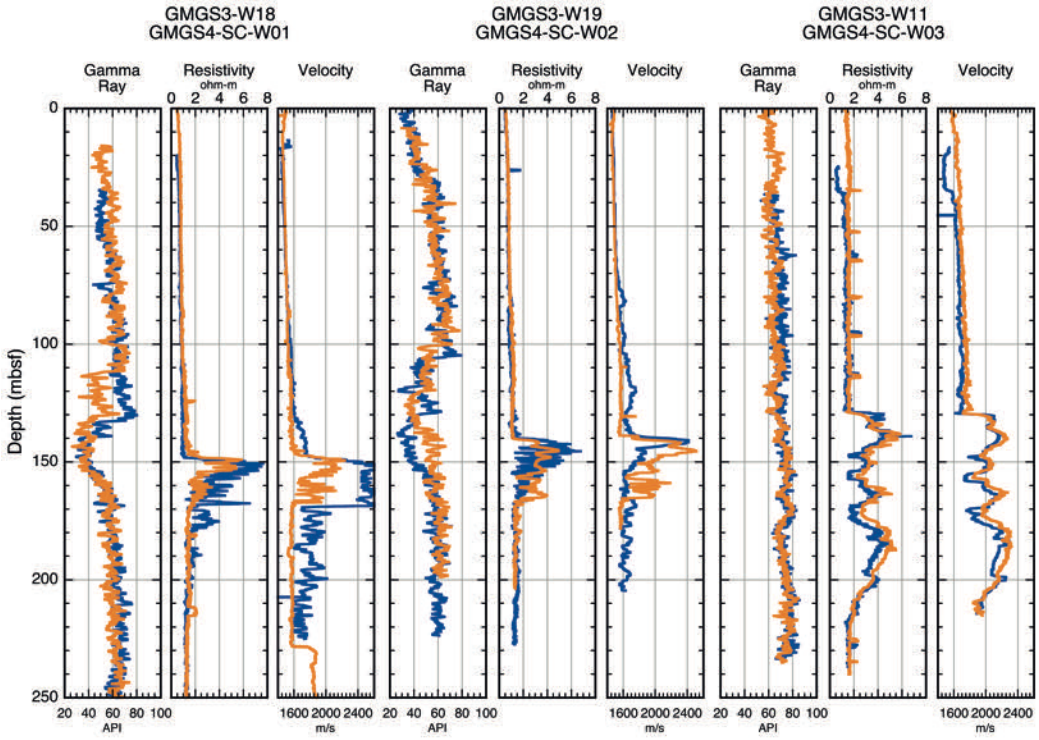

Figure 9: Comparison of downhole logging data from three locations visited twice. Blue line = GMGS3 data; orange line = GMGS4 data; dashed horizontal line = calculated base of gas hydrate stability (Structure I methane hydrate). Vertical offsets applied to data sets: GMGS3-W18 = 13.5m; GMGS4-SC-W02 = 5.7m; GMGS3-W11 = 16.5m.

Shenhu Gas Hydrate Further Questions

The most curious observation regarding the gas hydrate in the Shenhu area is also the most obvious one: gas hydrate exists at high concentrations (above 60%) in a uniform fashion between the grains of silty sediments. It immediately begs the question of how the gas hydrate got into these sediments, both on a grain scale and on an areal scale.

Many authors have suggested methods for moving gas vertically into the hydrate stability zone at Shenhu [35, 36, 37, 38, 39, 40], such as chimneys and fractures. In other fine-grained systems such as the Krishna-Godavari Basin [21], the Ulleung Basin [41], and the Dongsha area of the Pearl River Mouth Basin [42], gas moving along chimneys and fractures creates hydrate formations dominated by millimeter-scale subvertical hydrate veins, which may be created by gas/fluid fracturing of the sediment [43, 44]. Is the pore-filling morphology of the hydrate at the Shenhu area a result, then, of a different mode of gas delivery, or a much more permeable formation?

The Shenhu area is mainly silt, rather than clay [45, 29], with a median grain size of ~20 μm [46]. *In-situ* pore pressure dissipation measurements were made to determine *in situ* permeabilities both inside and outside of the gas

hydrate zone on Expedition GMGS4. The general background permeability of the sediments was near 2 mD outside of the gas-hydrate-bearing zone at most locations. Locations GMGS4-SC-W01 & -W02 had permeabilities within the gas-hydrate-bearing zone of 2 mD, with elevated readings (5-20 mD) just above and below the gas-hydrate-bearing zone. GMGS4-W07 had permeabilities of 20-40 mD inside the gas-hydrate-bearing zone, and GMGS4-SC-W03 had permeabilities of 5-40 mD inside and outside the gas-hydrate-bearing zone. Are these permeabilities high enough to convert fracture invasion to fluid flow?

Examining the gas hydrate distribution across the Shenhu area, the second outstanding feature is the sharp top of hydrate occurrence, which even exists at the recently active location. Su et al. [36] proposed that there are two main units in the upper Shenhu sediments, a lower unit composed of fine-grained turbidites, and an upper unit of poorly-sorted fine-grained sediments related to slope failures or other soft sediment deformational processes. Su et al. [36] further proposed that the turbidite unit might preferentially host gas hydrate in the Shenhu area, with the upper deformation unit acting as a seal. If this is the case, do the tops of the gas hydrate coincide with the upper/lower unit boundary?

The Shenhu drilling area has many features that make it a good region to test hypotheses surrounding hydrate formation. The unusual but uniform nature of the hydrate occurrence allows small changes in environment to be examined to see how the hydrate emplacement has been affected. The subregion with higher thermogenic input and recently active hydrate formation poses an exciting dichotomy: though the geochemistry (Figs. 4 & 8) looks distinct from other sites, the geophysical data (Fig. 9) look extremely similar. The deceptively simple Shenhu area could be a fascinating natural laboratory for understanding gas hydrate formation.

Acknowledgements

The authors would like to thank the crews of the D/V Bavenit & D/V Fugro Voyager and the science parties of Expeditions GMGS1, GMGS3 & GMGS4 for making these expeditions a success.

References

[1] H.Q. Zhang, S.X. Yang, N.Y. Wu, X. Xu, M. Holland, P. Schultheiss, K. Rose, H. Butler, G. Humphrey, GMGS-1 Science Team, “Successful and surprising results for China's first gas hydrate drilling expedition”. *Fire in the Ice*, Methane Hydrate Newsletter, National Energy Technology Laboratory, US Department of Energy, Fall issue 1, 2007.

[2] S.X. Yang, H.Q. Zhang, N.Y. Wu, X. Su, P. Schultheiss, M. Holland, G.X. Zhang, J.Q. Liang, J.A. Lu, K. Rose, “High concentration hydrate in disseminated forms obtained in Shenhu area, north slope of South China Sea”, *Proc. 6th Int. Conf. Gas Hydrates* (ICGH 2008), July 6-10, Vancouver, British Columbia, Canada, 10 pp., 2008.

[3] N.Y. Wu, H.Q. Zhang, S.X. Yang, G.X. Zhang, J.Q. Liang, J.G. Lu, X. Su, P. Schultheiss, M. Holland, Y.H. Zhu, “Gas Hydrate System of Shenhu Area, Northern South China Sea: Geochemical Results,” *Journal of Geological Research*, vol. 2011, Article ID 370298, 10 pp, doi:10.1155/2011/370298, 2011.

[4] H.S. Yu, “The Pearl River mouth basin: a rift basin and its geodynamic relationship with the southeastern Eurasian margin”, *Tectonophysics*, 183, 177-186, 1990.

[5] T. Lüdmann, H.K. Wong, “Neotectonic regime on the passive continental margin of the northern South China Sea”, *Tectonophysics*, 311, 113-138, 1999.

[6] X. Pang, C. Chen, D. Peng, M. Zhu, Y. Shu, M. He, J. Shen, B. Liu, “Sequence stratigraphy of deep-water fan system of Pearl River, South China Sea”, *Earth. Sci. Front.* 14(1), 220–229. doi:10.1016/ s1872-5791(07)60010-4, 2007.

[7] G. Gao, W. Gang, G. Zhang, W. He, X. Cui, H. Shen, S. Miao, “Physical simulation of gas reservoir formation in the Liwan 3-1 deep-water gas field in the Baiyun sag, Pearl River Mouth Basin”, *Natural Gas Industry B*, 2, 77-87, 2015.

[8] Q.X. Zhang, B.J. Huang, “Genetic types and generation history of natural gases from major basins in the South China Sea” (in Chinese), *China Offshore Oil & Gas*, 4, 5-13, 1991.

[9] B.J. Huang, X.M. Xiao, X.X. Li, “Geochemistry and origins of natural gases in the Yinggehai and Qiongdongnan Basins, Offshore South China Sea”, *Org Geochem*, 34, 1009–1025, 2003

[10] W.W. Ding, J.B. Li, J. Li, Y.X. Fang, Y. Tang, “Morphotectonics and evolutionary controls on the Pearl River Canyon system, South China Sea”, *Marine Geophysical Research*, 34, 221-238, 2013.

[11] C.L. Gong, Y.M. Wang, W.L. Zhu, W. Li, Q. Xu, Upper Miocene to Quaternary unidirectionally migrating deep-water channels in the Pearl River Mouth Basin, northern South China Sea”, *American Association of Petroleum Geologists Bulletin*, 97, 285-308, 2013.

[12] M.Z. Zhu, S. Grahamb, X. Pang, T. McHargue, “Characteristics of migrating submarine canyons from the middle Miocene to present: Implications for paleoceanographic circulation, northern South China Sea”, *Marine and Petroleum Geology*, 27:307-309, 2010.

[13] M. Su, R. Yang, C.M. Zhang, X.R. Cong, J.Q. Liang, Z.B. Sha, “Progress in study of deep-water depositional system in the northern continental slope of the South China Sea and its implications for gas hydrate research” (in Chinese with English abstract), *Marine Geology & Quaternary Geology*, 33, 109-116, 2013.

[14] D.W. Wang, S.G. Wu, Z.L. Qin, W.W. Ding, Q.B. Cao, “Architecture and identification of large Quaternary mass transport depositions in the slope of South China Sea” (in Chinese with English abstract). *Marine Geology & Quaternary Geology*, 29, 65-72. 2009.

[15] P. Schultheiss, J. Roberts, M. Druce, J. Priest, M. Holland, K. Yamamoto, S. Yang. PCATS and PCATS Triaxial: Further Development and Recent Field Experience Making Core Measurements Under Pressure. *Proceedings of the 8th International Conference on Gas Hydrates (ICGH 2014), Beijing, China, July 29-Aug 2,* 2014.

[16] P. Tishchenko, C. Hensen, K. Wallmann, C.S. Wong, "Calculation of the stability and solubility of methane hydrate in seawater", *Chemical Geology*, 27, 1197-1203, 2005.

[17] C. Liu, Y. Ye, Q. Meng, X. He, H. Lu, J. Zhang, J. Liu, S. Yang, “The characteristics of gas hydrates recovered from Shenhu Area in the South China Sea”, *Marine Geology*, 307-310, 22-27, 2012.

[18] A. Malinverno, M. Kastner, M.E. Torres, U.G. Wortmann, “Gas hydrate occurrence from pore water chlorinity and downhole logs in a transect across the northern Cascadia Margin (Integrated Ocean Drilling Program Expedition 311)”, *Journal of Geophysical Research-Solid Earth*, B08103 ,doi: 10.1029/2008JB005702, 2008.

[19] A.M. Tréhu, G. Bohrmann, FR Rack, Expedition 204 Scientists, *Proceedings of the Ocean Drilling Program: Volume 204 Initial Reports, Drilling Gas Hydrates on Hydrate Ridge, Cascadia Continental Margin*, Washington, DC: IODC Management International, Inc., http://www-odp.tamu.edu/publications/ 204_IR/ front.htm, 2004.

[20] M. Riedel, T.S. Collett, M.J. Malone, Expedition 311 Scientists. *Proceedings of the Ocean Drilling Program: Volume 311 Initial Reports*, Washington, DC: IODC Management International, Inc., doi:10.2204/iodp.proc. 311.109, 2006

[21] T.S Collett, M. Riedel, J. Cochran, R. Boswell, J. Presley, P. Kumar, A. Sathe, et al., *Indian National Gas Hydrate Program Expedition 01 Initial Reports: Expedition 01 of the Indian National Gas Hydrate Program from Mumbai, India to Chennai, India; Sites NGHP-01-01 through NGHP-01-21, April 2006–August 2006*, Initial Report, Directorate General of Hydrocarbons, Ministry of Petroleum and Natural Gas, Noida, India, 2008.

[22] P. Kumar, T. Collett, K. Vishwanath, K. Shukla, J. Nagalingam, M. Lall, Y. Yamada, P. Schultheiss and Holland, M., “Gas Hydrate-Bearing sand reservoir systems in the offshore of India: results of the India

National Gas Hydrate Program expedition 02". *Fire in the Ice (US DOE–NETL newsletter) Spring 2016,* pp. 1-8. Available online at: https://www.netl.doe.gov/File%20Library/Research/Oil-Gas/methane%20hydrates/MHNews_2016

[23] J.H. Kim, M.E. Torres, W.L. Hong, J.Y. Choi, M. Riedel, J.J. Bahk, S.H. Kim, "Pore fluid chemistry from the Second Gas Hydrate Drilling Expedition in the Ulleung Basin (UBGH2): Source, mechanisms and consequences of fluid freshening in the central part of the Ulleung Basin, East Sea", *Marine and Petroleum Geology*, 47, 99-112, 2013.

[24] J.Y. Lee, J.W. Jung, M.H. Lee, J.J. Bahk, J. Choi, B.J. Ryu, P. Schultheiss, "Pressure core based study of gas hydrates in the Ulleung Basin and implication for geomechanical controls on gas hydrate occurrence", *Marine and Petroleum Geology*, 47, 85-98, 2013.

[25] W. Ussler, III, C.K. Paull, "Ion exclusion associated with marine gas hydrate deposits" In: C.K. Paull, W.P. Dillon, (Eds.) *Natural Gas Hydrates: Occurrence, Distribution, and Detection*, Geophys. Monogr. Ser., vol. 124, AGU, Washington, D. C., pp. 41–51, 2001.

[26] A. Hiruta, G.T. Snyder, H. Tomaru, R. Matsumoto, "Geochemical constraints for the formation and dissociation of gas hydrate in an area of high methane flux, eastern margin of the Japan Sea," *Earth Planet Sci. Lett.*, 279, 326–339, 2009.

[27] M. Holland, P. Schultheiss, J. Roberts, M. Druce, "Observed Gas Hydrate Morphologies in Marine Sediments", *6th ICGH conference in Vancouver, July 6-10, 2008.* See also: https://circle.ubc.ca/ handle/2429/1201, 2008

[28] W.J. Winters, W.F. Waite, D.H. Mason, L.Y. Gilbert, I.A. Pecher, "Methane gas hydrate effect on sediment acoustic and strength properties", *Journal of Petroleum Science and Engineering*, DOI:10.1016/j.petrol.2006.02.003, 56, 127-135, 2007.

[29] X.J. Wang, S. Wu. M. Lee, Y. Guo, S.X. Yang, J.Q. Liang, "Gas hydrate saturation from acoustic impedance and resistivity logs in the Shenhu area, South China Sea", *Marine and Petroleum Geology*, 28, 1625-1633, 2011.

[30] P. Jaiswal, S. Al-Bulushi, P. Dewangan, "Logging-while-drilling and wireline velocities: Site NGHP-01-10, Krishna–Godavari Basin, India", *Marine and Petroleum Geology*, 58, 331-338, 2014.

[31] A.E Cook, B.I. Anderson, A. Malinverno, S. Mrozewski, D.S. Goldberg, "Electrical anisotropy due to gas hydrate-filled fracture planes", *Geophysics*, 75, F173-F185. doi:10.1190/1.3506530, 2010.

[32] B.B. Bernard, J.M. Brooks, W.M. Sackett, "Natural gas seepage in the Gulf of Mexico", *Earth and Planetary Science Letters*, 31, 48-54, 1976.

[33] S.Y. Fu, J.A. Lu, "The characteristics and origin of gas hydrate in Shenhu area, South China Sea", *Marine Geology Letters*, 26, 1-10, 2010.

[34] E.D. Sloan, C.A. Koh, *Clathrate Hydrates of Natural Gases, 3rd edn*. Taylor & Francis/CRC Press, Boca Raton, 2008.

[35] X.J. Wang, T.S. Collett, M.W. Lee, S.X. Yang, Y. Guo, S. Wu, "Geological controls on the occurrence of gas hydrate from core, downhole log, and seismic data in the Shenhu area, South China Sea", *Marine Geology*, 357, 272–292, 2014.

[36] M. Su, R. Yang, H. Wang, Z. Sha, J. Liang, N. Wu, S. Qiao, X. Cong, "Gas hydrates distribution in the Shenhu area, northern South China Sea: comparisons between the eight drilling sites with gas- hydrate petroleum system", *Geologica Acta*, 14(2), 79-100, 2016.

[37] D.X. Chen, S. Wu, D.D. Dong, L. Mi, S.Y. Fu, H. Shi, "Focused fluid flow in the Baiyun Sag, northern South China Sea: implications for the source of gas in hydrate reservoirs", *Chinese Journal of Oceanology and Limnology*, 31, 178-189, 2013.

[38] Y. Sun, S.G. Wu, D.D. Dong, T. Lüdmann, Y.H. Gong, "Gas hydrates associated with gas chimneys in fine-grained sediments of the northern South China Sea", *Marine Geology*, 311-314, 32-40, 2012.

[39] L. Li, X.H. Lei, X. Zhang, G.X. Zhang, "Heat flow derived from BSR and its implications for gas hydrate stability zone in Shenhu Area of northern South China Sea", *Mar. Geophys. Res.*, 33, 77-87, 2012.

[40] Q. Sun, S. Wu, J. Cartwright, D.D. Dong, "Shallow gas and focused fluid flow systems in the Pearl River Mouth Basin, northern South China Sea", *Marine Geology*, 315-318, 1-14, 2012.

[41] G.Y. Kim, B. Narantsetseg, B.J. Ryu, D.G. Yoo, J.Y. Lee, H.S. Kim, M. Riedel, "Fracture orientation and induced anisotropy of gas hydrate-bearing sediments in seismic chimney-like-structures of the Ulleung Basin, East Sea", *Marine and Petroleum Geology*, 47, 182–194, 2013.

[42] G.X. Zhang, J.Q. Liang, J. Lu, S.X. Yang, M. Zhang, M. Holland, P. Schultheiss, X. Su, Z. Sha, H. Xu, Y. Gong, S.Y. Fu, L. Wang, Z. Kuang, "Geological features, controlling factors and potential prospects of the gas hydrate occurrence in the east part of the Pearl River Mouth Basin, South China Sea", *Marine and Petroleum Geology*, 67, 356–367, 2015.

[43] A.K. Jain, R. Juanes. "Preferential mode of gas invasion in sediments: Grain-scale mechanistic model of coupled multiphase fluid flow and sediment mechanics", *J. Geophys. Res.,* 114, B08101. doi: 10.1029/2008JB006002, 2009.

[44] R. Holtzman, M.L. Szulczewski, R. Juanes, "Capillary fracturing in granular media", *Physical Review Letters,* 108, 264504, DOI: 10.1103/PhysRevLett.108.264504, 2012.

[45] F. Chen, Y. Zhou, X. Su, G. Liu, H. Lu, J. Wang, "Gas hydrate saturation and its relation with grain size of the hydrate-bearing sediments in the Shenhu area of northern South China Sea" (in Chinese with English abstract), *Marine Geology and Quaternary Geology*, 31, 95-100, 2011.

[46] J. Liang, J. Wei, N. Bigalke, J. Roberts, P. Schultheiss, M. Holland, "Laboratory Quantification of Geomechanical Properties of Hydrate-Bearing Sediments in the Shenhu Area of the South China Sea at In-Situ Conditions", *Proceedings of the 9th International Conference on Gas Hydrates (ICGH 2017), Denver, USA, June 25-30, 2017*, 2017.